Possibility of transforming the electronic structure of one species of graphene adatoms into that of another by application of gate voltage: First-principles calculations

Kevin T. Chan, Hoonkyung Lee, and Marvin L. Cohen

Possibility of transforming the electronic structure of one species of graphene adatoms into that of another by application of gate voltage: First-principles calculations

Kevin T. Chan, Hoonkyung Lee, and Marvin L. Cohen

Department of Physics, University of California, Berkeley, California 94720 and
Materials Sciences Division, Lawrence Berkeley National Laboratory, Berkeley, California 94720

(Dated: August 2, 2011)

Graphene provides many advantages for controlling the electronic structure of adatoms and other adsorbates via gating. Using the projected density of states and charge density obtained from first-principles density functional periodic supercell calculations, we investigate the possibility of performing "alchemy" of adatoms on graphene, i.e., transforming the electronic structure of one species of adatom into that of another species by application of a gate voltage. Gating is modeled as a change in the number of electrons in the unit cell, with the inclusion of a compensating uniform background charge. Within this model and the generalized gradient approximation to the exchange-correlation functional, we find that such transformations are possible for K, Ca, and several transition metal adatoms. Gate control of the occupation of the p states of In on graphene is also investigated. The validity of the supercell approxmation with uniform compensating charge and the model for exchange and correlation is also discussed.

I. INTRODUCTION

Much scientific effort is directed towards finding ways to control the electronic properties of materials, thereby opening greater possbilities for understanding fundamental physics and developing practical applications. The application of an electric field via gate voltage is a widely used method for controlling electronic properties of a variety of materials. The most well-known example is the field-effect transistor, a fundamental unit of many modern electronic devices.

Over the past several decades, it has become possible to fabricate smaller and smaller systems with electronic properties that can be controlled by a gate voltage. Because a quantum dot or nanoparticle of size $\sim$100 nm exhibits quantum confinement effects, its total charge, and transport through it, can be controlled electron by electron.[1] The study of quantum dots has led to the observation of fascinating phenomena such as Coulomb blockade and the Kondo effect.[2,3]

Even smaller than such "artificial atoms", single atoms or small molecules would be the ultimate limit of systems whose electronic properties could be controlled. Recent experiments have reported attaining this limit in molecules,[4,5] atoms bonded to organic ligands,[6] or dopant atoms in Si,[7,8] by observing Coulomb blockade and Kondo effects. In such systems, engineering wavefunctions[7] and constructing qubits[9] are now a possibility.

Recently, the controllable ionization of a Co atom adsorbed on graphene using a back gate voltage was shown.[10] This experiment demonstrates that gated adsorbates on graphene have great potential as atomic-scale systems with controllable electronic properties. Furthermore, recent theoretical studies have suggested that oxygen diffusion on graphene[11] and fluorine chemical bonding[12] can be controlled with gate voltage. Graphene has many beneficial properties for control of the electronic structure of adsorbates.[13] Its two-dimensional lattice of carbon atoms offers a clean, structurally robust surface for the adsorption of a wide variety of atoms or molecules. Its surface is amenable to imaging techniques and applications in surface chemistry, unlike atoms embedded in bulk materials. Importantly, neutral graphene has a small, linear density of states (DOS) near the Fermi level (E_F), which enables a large shift of E_F when a gate voltage is applied.

Guided by the idea that a singly-ionized isolated atom is isoelectronic to one of its neighbors in the Periodic Table, we suggest that it is possible to transform, electronically, an adatom on graphene into another adatom by gate-controlled ionization. We use the term "alchemy" to refer to such a transformation. In a previous work, we investigated the ionization of adatoms on graphene using first-principles calculations, finding reasonable qualitative agreement with essential features of experiment.[14] In the present work, we use a similar approach to explore the possiblity of alchemy of adatoms on graphene via gating. Using plane-wave pseudopotential (PWPP) density functional calculations with the generalized gradient approximation (GGA) and periodic supercells, we find that alchemy-like transformations are possible for both s and d valence adatoms, as demonstrated for K, Ca, Co, Ni and Cu adatoms. In addition, the calculations show that the occupation of localized p states of an In adatom on graphene can also be controlled by gate voltage. We discuss some limitations of comparing our model to experimental results, with particular focus on the approximation for exchange and correlation, supercell size, and electrostatic effects of periodic supercell calculations.

II. METHOD

A. Details of calculation

We perform our calculations using the first-principles PWPP method[15] within the framework of spin-polarized density-functional theory (DFT),[16,17] as implemented in the Quantum-ESPRESSO package.[18] The GGA exchange-correlation functional of Perdew, Burke, and Ernzerhof is used.[19] Ultrasoft pseudopotentials[20] are employed to model the ion cores for C, Co, Ni, Cu, and In; norm-conserving pseudopotentials[21] are employed for K and Ca.[55] The $4s$ and $4p$ states for K and Ca, $4d$, $5s$, and $5p$ states for In, and $4s$ and $3d$ states for Co, Ni, and Cu are treated as valence states. Nonlinear core corrections[22] are included for K, Ca, Co, Ni, and In. The plane wave energy cutoff for the electronic valence states is 30 Ry for the wavefunctions and 240 Ry for the charge density for K and Ca on graphene, and 40 Ry and 240 Ry, respectively, for Co, Ni, Cu, and In.

For calculations involving transition metals (TM), the LDA+U method[23] is often applied to treat correlations among d electrons. Our main results, given in Section III A, are restricted to the plain GGA case (U=0). In Ref. 14, the LDA+U method was considered for Co on graphene, and it was found that for U=0 eV, a Co $3d$ state is present at E_F, while for a U of 2 eV or 4 eV, a Co $3s$ state is at E_F. In the present work, we further assess the importance of the approximation for exchange and correlation on the PDOS for gated Co, Ni, and Cu adatoms on graphene by performing LDA+U calculations using the implementation of Ref. 24. We use a U of 4 eV and pseudoatomic orbitals for the projections. The effects of the additional U are discussed in Section III C.

The calculational geometry consists of an adatom on graphene in a 6×6 supercell[25] with 72 C atoms and 1 adatom. The x and y directions are defined to be parallel to the graphene plane, while the z direction is perpendicular to the plane. The calculated lattice constant for graphene is $a = 2.463$ Å, and the unit cell height perpendicular to the graphene plane is $L_z = 15$ Å. The unit cell dimensions are kept fixed for all calculations. A $3 \times 3 \times 1$ Γ-centered grid is used to sample the Brillouin zone, and a 0.05 eV Gaussian smearing is used for the electronic occupations.

In all cases, the adatom is placed on the hollow (H) site, above the center of a hexagon formed by six C atoms. In previous studies using the GGA, the adatom on the H site was found to have lower energy than on the bridge (B, midpoint of C-C bond) or top (T, above C atom) sites for all adatoms except for Cu.[26–29]

We assume that the main effect of applying a gate voltage to adatoms on graphene is to change the total number of electrons in the system. We therefore model gating by adding electrons to or removing electrons from the unit cell. A compensating uniform background charge is added to cancel the divergence of the total energy for charged supercells.[30,31] The electric field of the applied gate voltage is not included, but its effects are estimated in Section III D.

The method used in this work is similar to that of Ref. 14. The main difference is that in the present work, for each doping level, all atomic positions are fully relaxed such that the force on each atom is less than 0.002 Ry/a.u.

B. Relation of model to experiments

We now discuss the relation of our model to experiments, expanding on several points made in Ref. 14. The experiment of Ref. 10 studied Co adatoms on graphene at low coverage ($\sim$ 1 Co/2000 C). At such coverages, the doping level required to ionize an adatom is within the experimentally accessible range for graphene on an SiO$_2$ substrate with back gate; the doping range for this setup is $\sim \pm 10^{13}$ e/cm^2. However, achieving such a low adatom coverage in supercell calculations would require a prohibitively large supercell for the graphene in-plane direction. A 6×6 supercell is computationally accessible, but calculations with such a supercell can be expected to differ in some ways from experimental studies in the low coverage limit. In the calculation, adatom-adatom interactions are not negligible, especially for charged cells. In addition, because of the high coverage, a large doping level of ± 2 e/cell, or $\sim \pm 10^{14}$ e/cm^2, is required to occupy/unoccupy adatom levels. Since there is charge transfer and doping, there are band filling errors in the supercell calculation as compared to the low coverage limit. Despite these issues, we believe that qualitative features of our calculation can give insight into experiments conducted at the low adatom coverage limit.

On the other hand, for experiments involving adatoms on graphene at higher coverages, the adatom-adatom interactions and large doping levels of the supercell calculation are physically relevant. Such large doping levels are not achievable for current experiments on graphene on SiO$_2$. However, doping levels as high as 4×10^{14} e/cm^2 have been achieved using an electrolytic gate.[32] Therefore, experimental observation of the DOS for the doping levels considered in this work are within the realm of possibility. However, in modeling large doping levels using supercell calculations with a uniform neutralizing background charge, electrostatic errors can be significant. Corrections for such errors are not included in the results of Section III A, but are estimated in Section III D. In summary, a quantitative comparison of supercell calculations with experiments with low adatom coverage would likely require very large supercells, but low

doping levels. For comparison to experments at high adatom coverage, supercell sizes and doping levels close to that of the present calculation are appropriate, but electrostatic corrections are more important than in the low coverage case. We believe that the present computationally feasible model provides qualitative results that are relevant to experiment and useful for future theoretical studies with improved computational methods.

III. RESULTS

A. Adatom alchemy within the GGA

1. K and Ca adatoms

We begin with the results for s valence adatoms. We find that K and Ca bind with heights of 2.57 Å and 2.34 Å above the graphene plane, respectively, in reasonable agreement with previous results.[26] The adatom height is defined to be the difference in z coordinate of the adatom (z_a) and the average z coordinate of the C atoms in graphene (z_g). Figure 1(a) shows the PDOS for K on graphene for zero doping. A distinct peak with predominantly K $4s$ character lies 0.8 eV above E_F and is unoccupied. This state exhibits little hybridization with the graphene p states, and may thus be considered an atomic-like state localized on the K adatom. The graphene p PDOS is nearly unmodified below and up to 1 eV above E_F. The Dirac point E_D of graphene is clearly seen and lies 0.7 eV below E_F. This result is consistent with ionic bonding with charge transfer of the $4s$ valence electron of K to the graphene sheet. The net magnetization of the adatom-graphene system is zero.

Figure 1(f) shows the PDOS for Ca on graphene for zero doping. As in the case of K, there are distinct peaks corresponding to Ca $4s$ atomic-like states that do not hybridize with graphene. However, for the Ca adatom, the spin-up and spin-down Ca $4s$ states are split by about 1.0 eV, with the spin-up state occupied and spin-down state unoccupied. In the graphene PDOS, E_D lies 0.6 eV below E_F; above E_F the graphene states are modified by hybridization with Ca $3d$ states. As in the K case, the Ca adatom transfers one electron to graphene, but it retains its other $4s$ valence electron.

We now consider the effect of doping on the PDOS of the adatom-graphene system. Figures 1(b) and 1(c) show the PDOS for K on graphene with dopings of $+1$ e and $+2$ e, respectively (all quoted doping levels are per unit cell). At $+1$ e doping, the atomic-like K $4s$ spin-up state becomes partially occupied, and the up and down states become split in energy. At $+2$ e doping, the spin-up state is completely occupied, with a splitting of 0.7 eV between up and down states. The result is the ionization of the K adatom. The ionization of adatoms on graphene was studied previously in calculations for Li and Co adatoms.[14] The PDOS plots in Figs. 1(d) and 1(e) show that the Ca adatom can be similarly ionized by removal of electrons. At -1 e doping, the Ca adatom $4s$ state is partially unoccupied; at -2 e doping, it is completely unoccupied, with degenerate spin-up and spin-down states.

The corresponding PDOS plots in the left- and right-hand sides of Fig. 1 show qualitatively similar adatom levels and occupations. The K adatom with $+2$ e doping (Fig. 1(c)) has a single valence electron in the spin-up state, with the spin-down state unoccupied, just as in the case of the Ca adatom with 0 e doping (Fig. 1(f)). The two cases differ somewhat in the level splittings and position of peaks relative to the graphene p states. In addition, the occupied adatom state for K with $+2$ e doping acquires somewhat more p character than the corresponding Ca state for 0 e doping. Nevertheless, we can consider a K adatom doped with electrons to be transformed into a "quasi-Ca" adatom. Similarly, according to the calculated PDOS, the hole doped Ca adatom is transformed into "quasi-K" (Figs. 1(a) and 1(d)).

We also look at similarities in the charge densities for K and Ca adatoms with corresponding doping levels. Figure 2 shows total valence charge density isosurfaces for K and Ca adatoms at different doping levels. In all cases, the planar isosurface for the charge density of graphene is clearly visible, while signifcant changes are seen in the charge density near the adatom as the doping is changed. For undoped K on graphene (Fig. 1(a) and 2(a)), the localized atomic-like $4s$ state is unoccupied, and thus there is no valence charge density on the adatom. However, doping to $+2$ e occupies the spin-up K adatom state (Fig. 1(c)), with corresponding increase in charge density on the adatom (Fig. 2(c)). This charge density isosurface plot resembles that of the Ca adatom on graphene for zero doping (Fig. 2(f)); in the latter case, the Ca adatom also has its spin-up atomic-like state occupied. Similarly, doping Ca on graphene to -2 e unoccupies the spin-up localized atomic-like state, reducing the charge density on the adatom (Fig. 2(d)) and making it similar to that of K on graphene with zero doping (Fig. 2(a)).
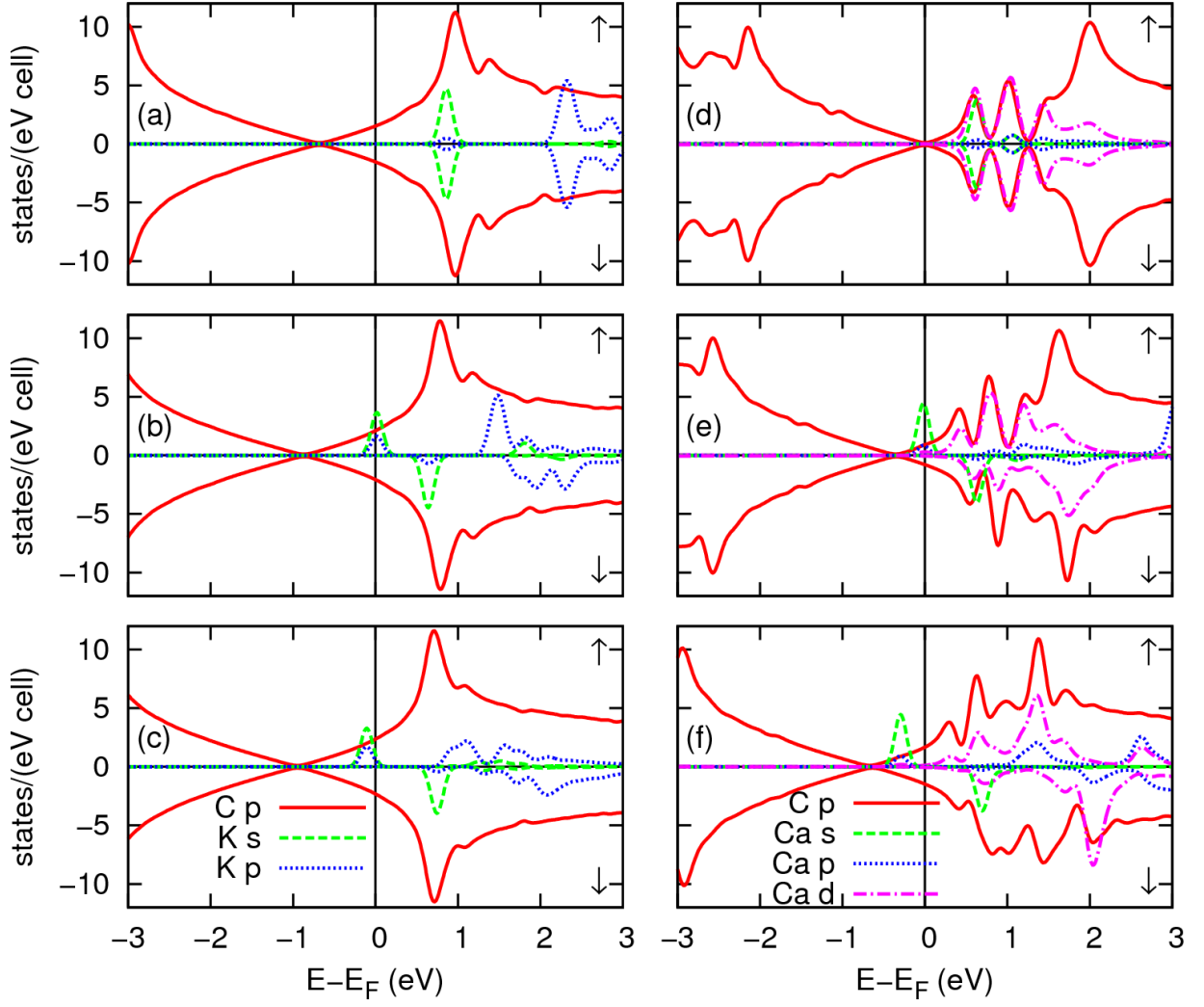
FIG. 1: (Color online) PDOS for K and Ca adatoms on graphene. Figures on the left are for K with doping levels (a) 0 e (b) +1 e (c) +2 e. Figures on the right are for Ca with doping levels (d) -2 e (e) -1 e (f) 0 e. Projections onto C $2p$ (solid red) and adatom $4s$ (dashed green), $4p$ (dotted blue), and $3d$ (dash-dotted magenta, Ca only) states are shown. Arrows indicate majority (up) and minority (down) spin channels. Energies are relative to the Fermi energy E_F.
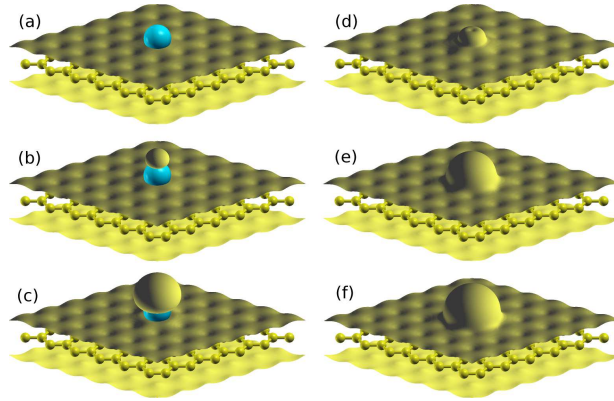

FIG. 2: (Color online) Isosurfaces of valence charge density for K and Ca adatoms on graphene. Figures on the left are for K with doping levels (a) 0 e (b) +1 e (c) +2 e. Figures on the right are for Ca with doping levels (d) -2 e (e) -1 e (f) 0 e. The isovalue is 0.001 e/a.u.^{3} for each plot.

TABLE I: Heights of adatoms above graphene sheet for different doping levels considered in this work. The $+/-$ signs in the adatom species headings denote addition/removal of electrons, with the doping amount indicated by the corresponding column under the "doping" heading.

doping (e)		height (Å)						
+	−	K (+)	Ca (−)	Co (+)	Ni (−)	Ni (+)	Cu (−)	In (+)
0	−2	2.57	2.19	1.54	1.61	1.55	1.82	2.51
+1	−1	2.58	2.27	1.48	1.58	1.57	1.81	2.50
+2	0	2.68	2.34	1.60	1.55	1.63	1.94	3.60

2. Transition metal adatoms

We now consider whether TM adatoms, possessing both d and s valence electrons, can be transformed electronically into other adatom species via gating. For 0 e doping, the calculated adsorption heights for Co, Ni, and Cu on the H site are 1.54, 1.55, and 1.94 Å, respectively, in reasonable agreement with previous results.[27–29] Although previous calculations report that Cu adsorption energies for the T or B sites are lower than for the H site,[28,29] for comparison we find it useful to model adsorption on the H site for all three adatoms.

Figures 3(a) and (f) show the PDOS at zero doping for Co and Ni on graphene, repsectively. In both cases, the $3d$ states of the adatom strongly hybridize with the graphene p states, while the adatom $4s$ states hybridize weakly with graphene. For Co, the $4s$ states are unoccupied, while there is approximately one hole in the $3d$ spin-down shell, and the system is spin-polarized. For Ni, the $3d$ shell is completely occupied, the $4s$ states are unoccupied, and the system is not spin-polarized.

In order to transform Co into Ni, the ionization of Co would have to fill the $3d$ shell, while transforming Ni to Co would require partially unoccupying the $3d$ shell. According to our calculations, the former does not occur, but the latter does. For Ni on graphene at -2 e doping (Fig. 3(d)), the occupation of the $3d$ state is in fact decreased, such that its electronic structure resembles that of undoped Co. As in the case of K and Ca, the relative positions of the atomic d and s states and graphene differ between neutral Co on graphene and doped Ni on graphene, but the ordering and occupations of the s- and d- derived adatom states are qualitatively similar. On the other hand, the Co $4s$ states lie close to E_F for the undoped system, so that when electrons are added, the occupations of both the Co $4s$ and $3d$ states are increased. At $+2e$ doping, the Co $4s$ and $3d$ states are partially occupied and lie at E_F, which is different from the case of the undoped Ni adatom.

While the transformation of Co to quasi-Ni upon doping does not occur in our calculations, we find that it is possible to transform Ni to quasi-Cu, and vice versa. Figure 4 shows the PDOS for various dopings for Ni and Cu. The $3d$ states lie far enough below E_F that their occupation is unchanged by doping. Instead, the occupation of the $4s$ spin-up states is varied by doping. In fact, tranformations between Ni and Cu are analogous to those between K and Ca, a main difference being that the $3d$ states are completely occupied in the TM case and completely unoccupied for the alkali/alkaline case.

3. In adatom

In addition to changing the occupation of s- and d-like adatom states by gating, it is also possible to change the occupation of p-like adatom states. For an In adatom on graphene at zero doping, the In $5p$ states hybridize with graphene and are somewhat broadened (Fig. 5(a)). The main peak lies 0.4 eV above E_F; these atomic-like states are spin-degnerate and unoccupied. Upon increasing the doping to $+2$ e (Fig. 5(c)), the spin-up $5p$ states become partially occupied, and the up and down states split in energy in a manner similar to that of the s states of a doped K adatom. However, one should take note of the large change in In adatom height for $+2$ e doping, as discussed in Section III B. Because of this large change in height, the adatom and graphene states are almost completely decoupled (Fig. 5(c)).

B. Effect of gating on atomic positions

In this section we discuss the effect that gating has on the positions of the graphene C atoms and the adatom. To quantify the displacement of C atoms from their position in pristine graphene, we define the distortion to be the maximum absolute difference between any C atom z coordinate and the average z coordinate of all the C atoms in
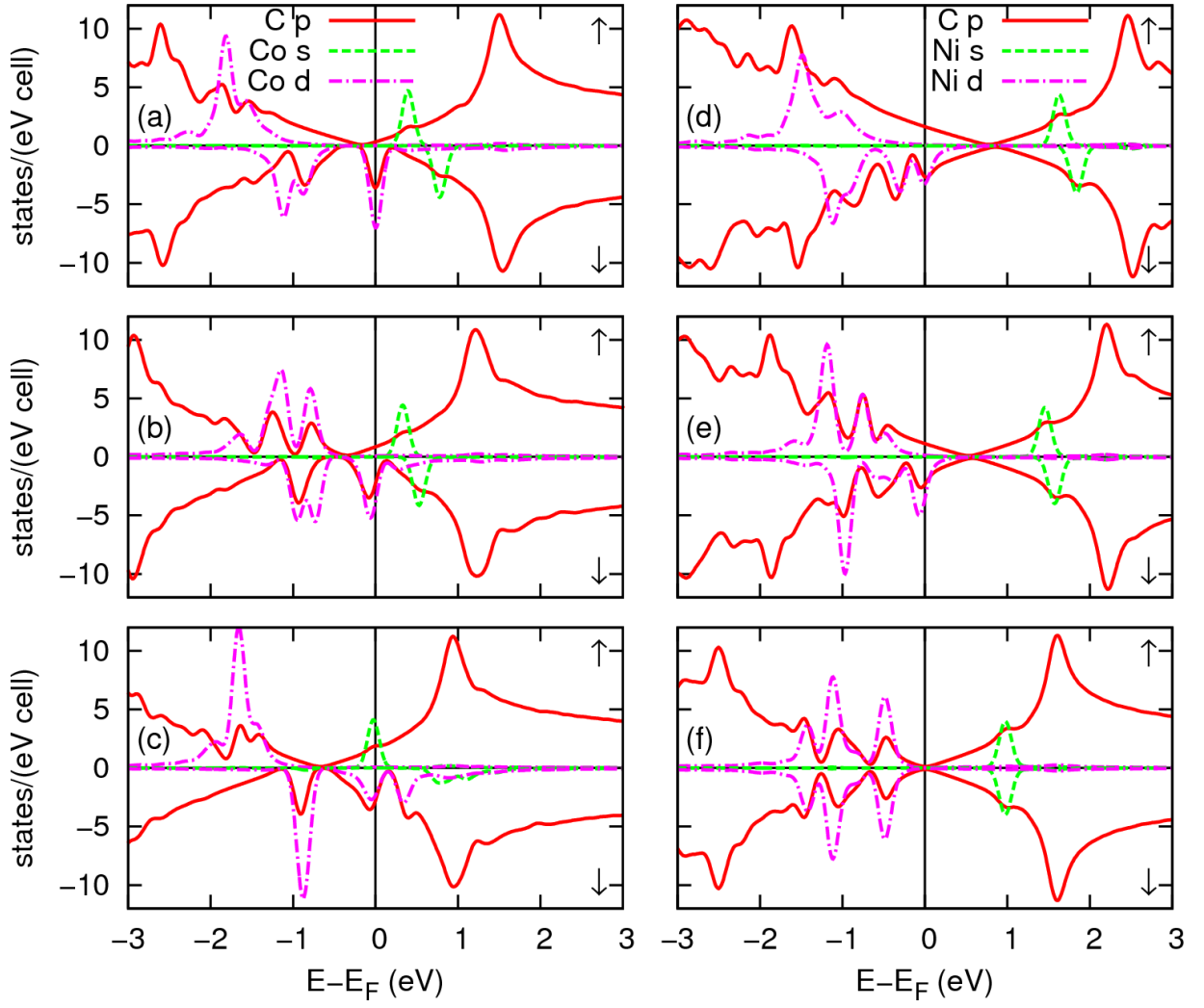
FIG. 3: (Color online) PDOS for Co and Ni adatoms on graphene. Figures on the left are for Co with doping levels (a) 0 e (b) +1 e (c) +2 e. Figures on the right are for Ni with doping levels (d) −2 e (e) −1 e (f) 0 e. Projections onto C 2p (solid red) and adatom 4s (dashed green) and 3d (dash-dotted magenta) states are shown. Arrows indicate majority (up) and minority (down) spin channels. Energies are relative to the Fermi energy E_F.

the graphene. For the undoped case, we find that the distortion is less than 0.01 Å for all the adatoms considered, consistent with previous results for adatoms on the H site of graphene.[26] With doping, the maximum distortion is less than 0.025 Å.

We do find changes in the position of the adatom relative to graphene as a function of doping. The adatom heights for the different doping levels considered in this work are presented in Table I. For most adatoms, the changes in height are about 0.1-0.2 Å; In is an exception.

An explanation for the trends in adatom height is suggested by the changes in occupation of adatom electronic levels as seen in the PDOS. For both K and Ca, an increase in adatom height correlates with an increase in the occupation of the adatom s orbital. A similar correlation holds for Ni when the doping is increased from 0 to +2 e and for Cu when the doping of is increased from −2 to 0 e. On the other hand, for Ni, an increase in adatom height is correlated with a decrease in occupation of adatom d states when going from 0 to −2 e doping. The case of Co is at first glance unusual, but it also follows the same trends. When the doping level is increased from 0 to +1 e, the occupation of Co d states is increased, and the adatom height decreases. Increasing the doping level from +1 to +2 e increases the occupation of the Co s state, and the adatom height increases.

We explain the correlation between adatom heights and occupancies of s or d states as follows. Adatom s states do not hybridize strongly with the C p states of graphene. When the occupation of the adatom s state is increased, the radius of the electronic cloud of the adatom is increased, pushing the adatom away from the graphene. On the other hand, adatom d states do hybridize strongly with C p states, forming covalent bonds. Increasing the occupation of
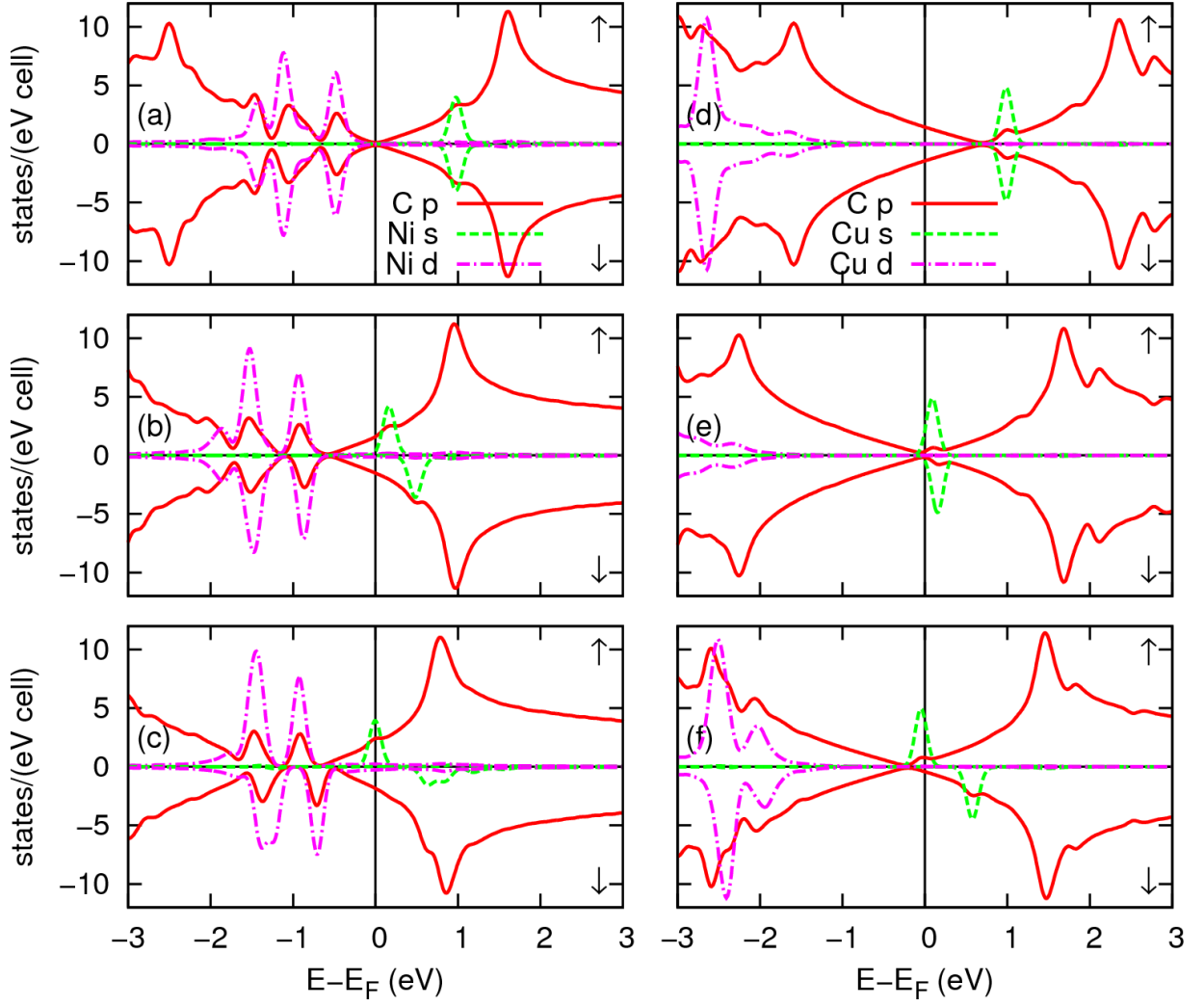
FIG. 4: (Color online) PDOS for Ni and Cu adatoms on graphene. Figures on the left are for Ni with doping levels (a) 0 e (b) +1 e (c) +2 e. Figures on the right are for Cu with doping levels (d) −2 e (e) −1 e (f) 0 e. Projections onto C 2p (solid red) and adatom 4s (dashed green) and 3d (dash-dotted magenta) states are shown. Arrows indicate majority (up) and minority (down) spin channels. Energies are relative to the Fermi energy E_F.

adatom d states strengthens the bond between the adatom and graphene and decreases the adatom height.

For In, the adatom height is increased by more than 1 Å when the doping is increased from +1 to +2 e. This result indicates that the binding of In is signifcantly weakened by this increase in doping. For In on graphene with zero doping, the binding has large ionic character, as indicated by the charge transfer from In to graphene, which leaves the In adatom positively charged. When the doping is increased to +2 e, In p states become filled, and the In adatom is no longer positively charged but rather close to neutral. Therefore the ionic bonding is significantly weakened.

A similar effect may happen for K. From 0 to +2 e doping, the K height is only increased by 0.11 Å, but for larger dopings the adatom height could increase and the binding could weaken even more. A more complete analysis of possible desorption of adatoms due to gating would be interesting but would need to take into account electrostatic errors in the potential and total energy for the supercell calculation with uniform neutralizing background.

We remark on the importance of relaxation of the atomic coordinates in the PDOS for gated adatoms. As a test, we calculate the PDOS for gated adatoms on graphene in which the C atoms are fixed to their positions in ideal, flat, two-dimensional graphene and the adatom height fixed to the optimized height for the undoped system, as in Ref. 14. We then compare these calculations to the calculations presented in Section III A for fully relaxed structures. Little qualitative difference is seen in most cases; the few noticeable differences can be explained by the change in adatom height. For example, in the calculation for the In adatom at +2 e doping with adatom height fixed to the optimized height for zero doping, there is adatom-graphene hybridization, but in the fully relaxed calculation, the hybridization is greatly reduced due to the increased adatom height. For all adatoms, the effect of the C lattice distortion on the
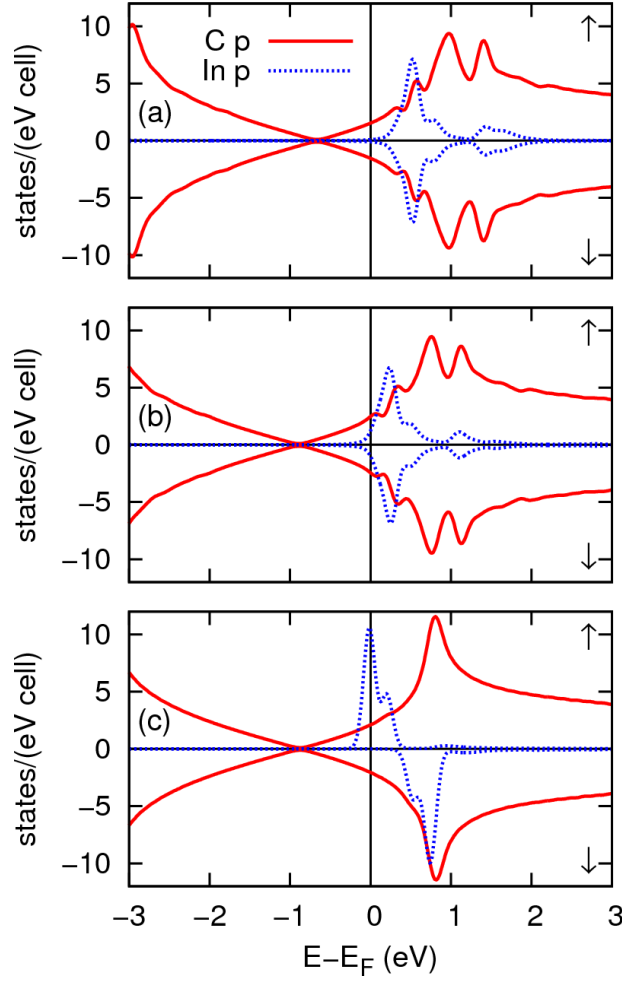
FIG. 5: (Color online) PDOS for an In adatom on graphene with doping levels (a) 0 e (b) +1 e (c) +2 e. Projections onto C $2p$ (solid red) and adatom $5p$ (dotted blue) states are shown (adatom $5s$ and $4d$ states lie outside the energy window). Arrows indicate majority (up) and minority (down) spin channels. Energies are relative to the Fermi energy E_F.

PDOS is small, which is reasonable given the small amount of distortion. We conclude that the main effect of the atomic relaxation is the change in adatom height. It is noted that the C lattice distortion may be more important for adatoms bound to the B or T sites.

C. Effect of Hubbard U

In this section, the effect of correlation in the $3d$ shell of TM adatoms, as modeled by the LDA+U method, is discussed. For Co on graphene, we find that for U=4 eV and a doping of 0 e, the T site is favored over the H site when all atoms are fully relaxed, in agreement with previous studies.[33] Furthermore, in Ref. 14, it was shown that for Co on the H site and U=2 or 4 eV, the DOS is changed qualitatively; a $4s$ rather than a $3d$ Co adatom state lies at E_F. Doping changes the occupation of the $4s$ state, in contrast to the U=0 eV case, for which the doping changes the $3d$ occupations. Since the results depend on the value of U, some doubt is cast on the U=0 eV result that Ni can be transformed into quasi-Co. It would be useful but beyond the scope of this study to determine whether a U of several eV or close to 0 eV is more appropriate to describe Co on graphene.

For Ni and Cu on graphene, we performed calculations for a doping of 0 e and U=4 eV. In both cases, the favored adsorption site was unchanged from the U=0 eV case (H for Ni and B for Cu). Furthermore, the DOS was qualitatively unchanged; the adatom $3d$ shell is completely filled (closed), and the $4s$ state is above (for Ni) or at (for Cu) E_F. We therefore expect that the results for doping of Ni or Cu on graphene will not be affected signifcantly by a U parameter that lies within this range.

D. Estimate of electrostatic errors in supercell calculations with uniform background charge

The use of periodic supercells to model charged systems can lead to unphysical effects that should be accounted for in calculations. In this Section, we describe our method of estimating these effects and discuss the implication of these effects on our results for the PDOS and atomic positions.

1. Method of estimation

An infinite lattice of periodically repeated charged supercells has a divergent total energy per unit cell. To get a finite total energy, a compensating charge must be added to the cell to make it neutral. In the present work, a uniform compensating charge is employed.[30,31] Such an approach is commonly used as it is automatically implemented in many plane-wave pseudopotential approaches.[15] However, the compensating charge is unphysical and can affect the electrostatic potential and total energy. Furthermore, the unphysical interaction between neutral periodic supercell images can also be significant.

In the present work, we determine a correction to the electrostatic potential and use this correction to estimate the effects on our results for the PDOS and atomic positions. We build upon the approach of Ref. 34 for charged slabs and additionally include dipole corrections.

As in Ref. 34, let ρ denote the charge density of the slab (in the present case, a graphene plane with adatoms) and $\tilde{\rho}$ denote the slab plus background charge density ρ_b:

$$\tilde{\rho}(\vec{r}) = \rho(\vec{r}) + \rho_b(\vec{r}), \tag{1}$$

where in the present case $\rho_b(\vec{r}) = -\langle\rho(\vec{r})\rangle$ is uniform (the angled brackets denote the average over the unit cell). Similarly, let V denote the electrostatic potential of the slab, $\widetilde{V}$ denote the electrostatic potential of the slab plus background charge density in periodic boundary conditions, and V_b denote the potential of the background charge:

$$\widetilde{V}(\vec{r}) = V(\vec{r}) + V_b(\vec{r}). \tag{2}$$

In analogy with the method of Ref. 35, let us define the corrective potential as

$$V_{\mathrm{corr}}(\vec{r}) = V(\vec{r}) - \widetilde{V}(\vec{r}), \tag{3}$$

so that $V_{\mathrm{corr}}(\vec{r}) = -V_b(\vec{r})$. Then Poisson's equation for the corrective potential is

$$\nabla^2 V_{\mathrm{corr}}(\vec{r}) = 4\pi\rho_b(\vec{r}). \tag{4}$$

We obtain the corrective potential by solving this equation with appropriate boundary conditions.

The potential $\widetilde{V}$ and charge density $\tilde{\rho}$ are solved for self-consistently using standard PWPP DFT methods. The corrective potential V_{corr} is added *a posteriori* to $\widetilde{V}$ to get the potential V of the slab in vacuum without any background charge. Therefore, the charge density $\tilde{\rho}$ and potential V are not consistent with each other. Some change in the charge density is expected if it is solved for self-consistently in the corrected potential V; the effects of this change in charge density on the PDOS and forces are expected to be small and are neglected.

In order to solve Poisson's equation for the corrective potential, we make a planar-average approximation[36] in which we assume that the corrective potential is uniform in the x-y plane and only varies in the z direction perpendicular to the graphene plane. Under this approximation, Poisson's equation is one-dimensional and can be solved if the boundary conditions are specified.

For a charged system with two-dimensional periodicity, such as a charged slab, the boundary conditions require some consideration. The potential of a uniformly charged infinite 2D plane relative to a point infinitely far away from it is infinite, so the zero of the potential energy cannot be defined as the vacuum level, as is often done for zero-dimensional charged systems. This issue can be dealt with by specifying a reference electrode,[34] a plane at a specified distance from the slab whose potential is defined to be zero. This distance should be large enough to ensure that the plane lies in a region of vacuum where the potential as a function of z is linear.

In addition to choosing the position of the reference electrode, the slope of the potential at the reference electrode must also be specified. In the present work, we consider two possible boundary conditions. Boundary condition 1 (BC1) is specified such that the electric fields far in the vacuum region on either side of the slab are equal in magnitude but opposite in sign. Such a boundary condition could be obtained in experiment with both back and top gates and appropriately tuned potential differences. For boundary condition 2 (BC2), the electric field is zero far in the vacuum region on the adatom side of the slab. The BC2 is relevant for experiments with a single back gate. The back gate

electrode contains an equal and opposite sign charge per unit area as the charged slab. For BC2, as for a parallel plate capacitor, a finite electric field exists in the region between the back gate electrode and the charged slab, and zero electric field exists in the vacuum region on the side of the slab facing away from the back gate.

With the boundary conditions specified, we solve for the corrective potential V_{corr}. Following Ref. 34, let q denote the net charge of the unit cell ($q > 0$ for excess electrons), A_0 the unit cell area in the graphene plane, z_0 a chosen origin, Λ the distance between the reference electrode and the origin ($\Lambda > 0$), L_z the length of the unit cell in the z direction, and p the dipole moment per unit cell in the z direction:

$$p = \int_{\mathrm{cell}} \rho(\vec{r}) z \, d\vec{r}. \tag{5}$$

For an origin chosen such that the dipole moment is zero, the corrective potential for BC1 was given in Ref. 34. We use V_{mon} to denote this "monopole" potential:

$$V_{\mathrm{mon}}(z) = \frac{2\pi q}{A_0} \left[\frac{(z - z_0)^2 - L_z \Lambda + (L_z/2)^2}{L_z} \right]. \tag{6}$$

If the dipole moment is not zero, we add to V_{mon} a dipole potential:[37,38]

$$V_{\mathrm{dip}}(z) = -\frac{4\pi p}{A_0} \frac{z - z_0}{L_z}, \tag{7}$$

so the corrective potential is given by

$$V_{\mathrm{corr}} = V_{\mathrm{mon}} + V_{\mathrm{dip}}. \tag{8}$$

The origin should be chosen such that $z_0 \pm L_z$ lies in the vacuum region, but aside from this criterion the precise choice does not affect the corrective potential. For any shift in the origin, the change in V_{mon} will be compensated for, aside from an overall constant, by a change in V_{dip} via a change in p. The overall constant is not important for the estimates given in the present work, but would be important if one needed to determine total energy differences for charged slabs. Likewise, the choice of reference electrode position is not particularly important in this work, so long as it lies in the vacuum region where the potential is linear.

The potential for BC2 can be obtained from the potential for BC1 by adding a linear potential, equivalent to adding a constant electric field perpendicular to the graphene plane:

$$V_{\mathrm{corr}} = V_{\mathrm{mon}} + V_{\mathrm{dip}} + V_{\mathrm{efield}}, \tag{9}$$

with

$$V_{\mathrm{efield}} = \frac{2\pi q}{A_0} (z - z_0). \tag{10}$$

As an example, the planar-averaged uncorrected electrostatic potential and corrected potentials for BC1 and BC2 for K on graphene with a doping level of $q = +2e$ are plotted in Fig. 6. The origin is chosen to be at 7.5 Å, near the position of the graphene plane. The reference electrode is chosen to be at 0 Å, so that $\Lambda = 7.5$ Å. For the 6×6 unit cell, $A_0 = 189.09$ Å^2, and $L_z = 15$ Å. The dipole moment is calculated to be $p = 3.45$ eÅ. As expected, the potential becomes linear at the edges of the unit cell for the corrected potentials; for BC1, the magnitudes of the slopes on either side of the graphene plane are equal, while for BC2, the slope is zero on the adatom side of the graphene plane.

After computing the corrective potential V_{corr}, we can estimate the effect of this potential on the PDOS and atomic positions. For the PDOS, we might expect the potential to shift the positions of the adatom states relative to the graphene states. For a rough estimate of this shift, we assume that the graphene states lie at the position of the graphene plane z_g, while the adatom states lie at the position of the adatom z_a. In reality these states have some z distribution, but our simple assumption gives a reasonable estimate. The estimate for the relative energy shift is given by $\Delta\epsilon = V_{\mathrm{corr}}(z_a) - V_{\mathrm{corr}}(z_g)$.

For the atomic positions, we estimate the force on the adatom, F^a_{corr}, and the graphene plane, F^g_{corr}, due to V_{corr}. We have

$$F^a_{\mathrm{corr}} = -Q_a \frac{d}{dz} V_{\mathrm{corr}}(z)|_{z = z_a}, \tag{11}$$

and similarly for F^g_{corr}. To estimate the net charge Q_a of the adatom we take the difference of the Löwdin electron charge[39] and the ion core charge. The same is done for the C atoms and then averaged over all the atoms in graphene to get the net charge Q_g. The force on the graphene plane turns out to be small in comparison to the force on the adatom, so F^g_{corr} can be neglected in our estimates. The force can be translated into a change in the adatom height above the graphene sheet by assuming a harmonic potential of a given curvature between the adatom and graphene. We neglect the additional change in PDOS that this change in adatom position would cause.
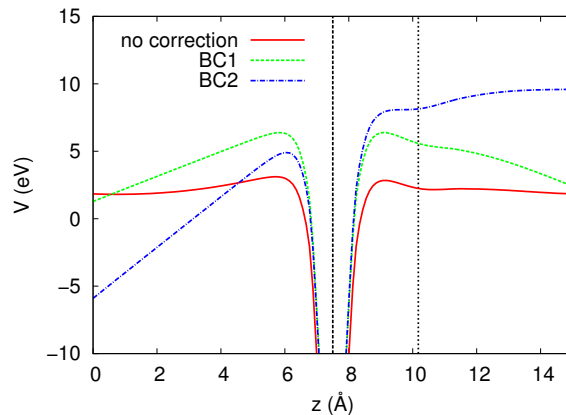
FIG. 6: (Color online) Planar-averaged uncorrected electrostatic potential (solid red) and corrected potentials for boundary condition 1 (dashed green) and boundary condition 2 (dash-dotted blue) for K on graphene with doping level of $+2$ e/cell. The vertical dashed and dotted black lines denote the graphene and adatom z positions, respectively.

2. Estimation results

For BC1, we find that $|\Delta\epsilon| < 0.1$ eV for most adatoms and doping levels. One exception is K, for which $\Delta\epsilon \sim -0.3$ eV. Also, in the case of In, $\Delta\epsilon \sim -0.5$ eV for $q = +2e$; the large shift is related to the large adatom height of 3.60 Å. Although these shifts in the PDOS might change the precise values of the doping levels at which states are occupied or unoccupied, they do not appear large enough to change qualitatively our main results concerning adatom alchemy.

As for the forces under BC1, in all cases, $|F^a_{\mathrm{corr}}| < 0.2$ eV/Å. As a rough estimate, assuming an out-of-plane adatom vibration mode energy of ~ 10 meV (Ref. 10) and using an atomic mass of ~ 40 (for K), a force of 0.2 eV/Å gives a displacement of ~ 0.2 Å.

From these estimates, we can conclude that our model consisting of a charged adatom on graphene in a periodic supercell with neutralizing background gives qualitatively reasonable results for the physical system with BC1. Electrostatic corrections at least to dipole order should be included to get quantitative results to ~ 0.1 Å precision in adatom position and ~ 0.1 eV precision in the PDOS.

The applied electric field which provides the difference in potential between BC1 and BC2 is close to 1 eV/Å for a doping level of $\pm\,2$ e. Such a large electric field leads to estimates of $|\Delta\epsilon| \sim 1$ eV for DOS energy shifts and $|F^a_{\mathrm{corr}}| \sim 1$ eV/Å for force corrections. Therefore, the model used in the present calculations is not adequate for a system with BC2 at these doping levels; explicit inclusion of the electric field is important and has a signifcantly larger effect than the inclusion of potentials V_{mon} and V_{dip}.

Despite this difference, our results still have relevance for experiments for gated adatoms on graphene in which both the adatom coverage and the doping level are significantly reduced (by an order of magnitude). In such cases, the electric field due to the back gate is reduced in proportion to the doping level, and the corrections are smaller. As noted in Section II B, the different adatom coverage between our calculation and such experiments should be taken into account when comparing the two.

We mention several references that have addressed aspects of charged supercell calculations relevant to the present work. A monopole and dipole potential correction similar to the one given here and implemented self-consistently is described in Ref. 40. A more general scheme to compute the full corrective potential for a charged system in uniform neutralizing background is given in Ref. 35. A Green's function approach for charged slabs that can include an "effective screening medium" is detailed in Ref. 41. A somewhat different approach to dealing with charged supercells is to explicitly model a countercharge of computationally advantageous shape.[42–44] Several studies have applied this approach to charged slab geometries.[45–52]

IV. CONCLUSION

The controlled "alchemy" of adatoms, as explored in this work, could have significant applications. Many chemical reactions rely on TM catalysts, which may be difficult to control. One could imagine transforming, via gating, adatoms which are easier to deal with experimentally but less useful chemically into other adatoms that can catalyze important reactions. We have investigated this tranformation for certain adatoms, but it may be possible for other species as

well; this possibility warrants future study. Graphene coated with Ca or TM adatoms is also a possible material for hydrogen storage.[53] Gating such adatom-graphene materials might allow for controlled adsorption/desorption of hydrogen.

In summary, the gate-controlled alchemy of adatoms on graphene is explored using first-principles density functional supercell calculations with the GGA. Transformations between K and Ca, between Ni and Cu, and of Ni to Co are demonstrated. The gating of In adatoms is also studied. Changes in adatom height with gating are explained by comparison with the PDOS. The inclusion of a Hubbard U to model correlation in $3d$ states of adatoms can have a significant effect on the results. Also, electrostatic corrections to the supercell approximation with uniform background charge are important for obtaining quantitative results for large amounts of doping. We therefore caution against interpreting our results as definitive predictions of adatom alchemy. Nevertheless, we hope that this work will stimulate further theoretical and experimental study of the phenomenon of adatom alchemy on graphene via application of gate voltage.

Acknowledgments

[1] M. A. Kastner, Rev. Mod. Phys. **64**, 849 (1992).

[2] D. Goldhaber-Gordon, H. Shtrikman, D. Mahalu, D. Abusch-Magder, U. Meirav, and M. A. Kastner, Nature **391**, 156 (1998).

[3] S. M. Cronenwett, T. H. Oosterkamp, and L. P. Kouwenhoven, Science **281**, 540 (1998).

[4] W. Liang, M. P. Shores, M. Bockrath, J. R. Long, and H. Park, Nature **417**, 725 (2002).

[5] S. Kubatkin, A. Danilov, M. Hjort, J. Cornil, J.-L. Bredas, N. Stuhr-Hansen, P. Hedegard, and T. Bjornholm, Nature **425**, 698 (2003).

[6] J. Park, A. N. Pasupathy, J. I. Goldsmith, C. Chang, Y. Yaish, J. R. Petta, M. Rinkoski, J. P. Sethna, H. D. Abruna, P. L. McEuen, et al., Nature **417**, 722 (2002).

[7] G. P. Lansbergen, R. Rahman, C. J. Wellard, I. Woo, J. Caro, N. Collaert, S. Biesemans, G. Klimeck, L. C. L. Hollenberg, and S. Rogge, Nat. Phys. **4**, 656 (2008).

[8] G. P. Lansbergen, G. C. Tettamanzi, J. Verduijn, N. Collaert, S. Biesemans, M. Blaauboer, and S. Rogge, Nano Lett. **10**, 455 (2010).

[9] A. Morello, J. J. Pla, F. A. Zwanenburg, K. W. Chan, K. Y. Tan, H. Huebl, M. Mottonen, C. D. Nugroho, C. Yang, J. A. van Donkelaar, et al., Nature **467**, 687 (2010).

[10] V. W. Brar, R. Decker, H.-M. Solowan, Y. Wang, L. Maserati, K. T. Chan, H. Lee, C. O. Girit, A. Zettl, S. G. Louie, et al., Nat Phys **7**, 43 (2011).

[11] A. M. Suarez, L. R. Radovic, E. Bar-Ziv, and J. O. Sofo, Phys. Rev. Lett. **106**, 146802 (2011).

[12] J. O. Sofo, A. M. Suarez, G. Usaj, P. S. Cornaglia, A. D. Hernández-Nieves, and C. A. Balseiro, Phys. Rev. B **83**, 081411 (2011).

[13] A. K. Geim and K. S. Novoselov, Nat. Mater. **6**, 183 (2007).

[14] K. T. Chan, H. Lee, and M. L. Cohen, Phys. Rev. B **83**, 035405 (2011).

[15] J. Ihm, A. Zunger, and M. L. Cohen, J. Phys. C: Solid State Phys. **12**, 4409 (1979).

[16] P. Hohenberg and W. Kohn, Phys. Rev. **136**, B864 (1964).

[17] W. Kohn and L. J. Sham, Phys. Rev. **140**, A1133 (1965).

[18] P. Giannozzi, S. Baroni, N. Bonini, M. Calandra, R. Car, C. Cavazzoni, D. Ceresoli, G. L. Chiarotti, M. Cococcioni, I. Dabo, et al., J. Phys. Condens. Matter **21**, 395502 (2009).

[19] J. P. Perdew, K. Burke, and M. Ernzerhof, Phys. Rev. Lett. **77**, 3865 (1996).

[20] D. Vanderbilt, Phys. Rev. B **41**, 7892 (1990).

[21] N. Troullier and J. L. Martins, Phys. Rev. B **43**, 1993 (1991).

[22] S. G. Louie, S. Froyen, and M. L. Cohen, Phys. Rev. B **26**, 1738 (1982).

[23] V. I. Anisimov, F. Aryasetiawan, and A. I. Lichtenstein, Journal of Physics: Condensed Matter **9**, 767 (1997).

[24] M. Cococcioni and S. de Gironcoli, Phys. Rev. B **71**, 035105 (2005).

[25] M. L. Cohen, M. Schlüter, J. R. Chelikowsky, and S. G. Louie, Phys. Rev. B **12**, 5575 (1975).

[26] K. T. Chan, J. B. Neaton, and M. L. Cohen, Phys. Rev. B **77**, 235430 (2008).

[27] Y. Yagi, T. M. Briere, M. H. F. Sluiter, V. Kumar, A. A. Farajian, and Y. Kawazoe, Phys. Rev. B **69**, 075414 (2004).

[28] H. Valencia, A. Gil, and G. Frapper, J. Phys. Chem. C **114**, 14141 (2010).

[29] C. Cao, M. Wu, J. Jiang, and H.-P. Cheng, Phys. Rev. B **81**, 205424 (2010).

[30] M. Leslie and N. J. Gillan, Journal of Physics C: Solid State Physics **18**, 973 (1985).

[31] G. Makov and M. C. Payne, Phys. Rev. B **51**, 4014 (1995).

[32] D. K. Efetov and P. Kim, Phys. Rev. Lett. **105**, 256805 (2010).

[33] T. O. Wehling, A. V. Balatsky, M. I. Katsnelson, A. I. Lichtenstein, and A. Rosch, Phys. Rev. B **81**, 115427 (2010).

[34] A. Y. Lozovoi, A. Alavi, J. Kohanoff, and R. M. Lynden-Bell, The Journal of Chemical Physics **115**, 1661 (2001).

[35] I. Dabo, B. Kozinsky, N. E. Singh-Miller, and N. Marzari, Phys. Rev. B **77**, 115139 (2008).

[36] A. Baldereschi, S. Baroni, and R. Resta, Phys. Rev. Lett. **61**, 734 (1988).

[37] J. Neugebauer and M. Scheffler, Phys. Rev. B **46**, 16067 (1992).

[38] L. Bengtsson, Phys. Rev. B **59**, 12301 (1999).

[39] P.-O. Löwdin, **18**, 365 (1950).

[40] P. Gava, M. Lazzeri, A. M. Saitta, and F. Mauri, Phys. Rev. B **79**, 165431 (2009).

[41] M. Otani and O. Sugino, Phys. Rev. B **73**, 115407 (2006).

[42] P. A. Schultz, Phys. Rev. B **60**, 1551 (1999).

[43] P. A. Schultz, Phys. Rev. Lett. **84**, 1942 (2000).

[44] P. E. Blochl, The Journal of Chemical Physics **103**, 7422 (1995).

[45] C. L. Fu and K. M. Ho, Phys. Rev. Lett. **63**, 1617 (1989).

[46] K. P. Bohnen and D. M. Kolb, Surface Science **407**, L629 (1998).

[47] S. Heinze, X. Nie, S. Blgel, and M. Weinert, Chemical Physics Letters **315**, 167 (1999).

[48] A. Y. Lozovoi and A. Alavi, Phys. Rev. B **68**, 245416 (2003).

[49] J.-S. Filhol and M. Neurock, Angewandte Chemie **118**, 416 (2006).

[50] S. Kajita, T. Nakayama, and J. Yamauchi, Journal of Physics: Conference Series **29**, 120 (2006).

[51] C. D. Taylor, S. A. Wasileski, J.-S. Filhol, and M. Neurock, Phys. Rev. B **73**, 165402 (2006).

[52] S. Schnur and A. Groß, Catalysis Today **165**, 129 (2011).

[53] H. Lee, J. Ihm, M. L. Cohen, and S. G. Louie, Nano Lett. **10**, 793 (2010).

[54] A. Kokalj, Computational Materials Science **28**, 155 (2003).

[55] We used the pseudopotentials C.pbe-rrkjus.UPF, Co.pbe-nd-rrkjus.UPF, Ni.pbe-nd-rrkjus.UPF, Cu.pbe-d-rrkjus.UPF, and In.pbe-d-rrkjus.UPF from http://www.quantum-espresso.org. Pseudopotentials for K and Ca were generated using the Quantum-ESPRESSO package.